Reprinted from

MATERIALS LETTERS

AN INTERDISCIPLINARY JOURNAL AFFILIATED WITH THE **MATERIALS RESEARCH SOCIETY** AND THE **MATERIALS RESEARCH SOCIETY-JAPAN** DEVOTED TO THE RAPID PUBLICATION OF SHORT COMMUNICATIONS ON THE SCIENCE, APPLICATIONS AND PROCESSING OF MATERIALS

Materials Letters 36 (1998) 179–185

Synthesis of lead zirconate powders via a polyaniline-mediated microemulsion processing route

Jiye Fang [a], John Wang [a,*], Ser-Choon Ng [b], Leong-Ming Gan [c,d,1], Chai Hoon Quek [c], Chwee-Har Chew [c]

[a] *Department of Materials Science, National University of Singapore, Singapore 119260, Singapore*
[b] *Department of Physics, National University of Singapore, Singapore 119260, Singapore*
[c] *Department of Chemistry, National University of Singapore, Singapore 119260, Singapore*
[d] *IMRE, National University of Singapore, Singapore 119260, Singapore*

Received 30 December 1997; accepted 13 January 1998

ELSEVIER

July 1998

ELSEVIER

Materials Letters 36 (1998) 179–185

MATERIALS LETTERS

Synthesis of lead zirconate powders via a polyaniline-mediated microemulsion processing route

Jiye Fang [a], John Wang [a,*], Ser-Choon Ng [b], Leong-Ming Gan [c,d,1], Chai Hoon Quek [c], Chwee-Har Chew [c]

[a] *Department of Materials Science, National University of Singapore, Singapore 119260, Singapore*
[b] *Department of Physics, National University of Singapore, Singapore 119260, Singapore*
[c] *Department of Chemistry, National University of Singapore, Singapore 119260, Singapore*
[d] *IMRE, National University of Singapore, Singapore 119260, Singapore*

Received 30 December 1997; accepted 13 January 1998

Abstract

Oxalate precursors of lead zirconate were synthesised in the nanosized aqueous domains of an inverse microemulsion consisting of cyclohexane, NP5 + NP9 and an aqueous phase of mixed lead and zirconium nitrates. Polyaniline was added into the microemulsion-derived precursor via an in-situ polymerisation in the aqueous phase when lead oxalate and zirconium oxalate are coprecipitated. The in-situ polymerisation of anilines in the microemulsion resulted in the formation of a well dispersed precursor powder, after the nanosized oxalate particles were retrieved from the reacted microemulsions by repeated washing using distilled ethanol. Upon calcination at 800°C, the microemulsion-derived oxalate precursor led to the formation of an ultrafine lead zirconate powder, which was characterised for various powder characteristics.

Keywords: Lead zirconate; Microemulsion; Coprecipitation; Ultrafine powder; Powder synthesis; Ceramics

1. Introduction

Lead zirconate (PZ) exhibits an orthorhombic structure at room temperature and transforms to cubic at around 230°C [1]. It has been extensively studied because of its unique pyroelectric, electrooptical [2,3], and piezoelectric properties [1,4–7], which are required for many applications in electronics and microelectronics [8,9]. Lead zirconate is also a candidate material for energy storage applications [10] due to its antiferroelectric to ferroelectric transition, as well as an important source material for the fabrication of lead zirconate titanate (PZT) [11]. PZ powders and sintered PZ ceramics have been synthesised via various ceramic and chemistry-based novel processing routes [11–14].

Among the chemistry-based novel processing routes developed for the preparation of fine functional ceramic powders, microemulsion processing [15–17] is superior to many others in terms of being able to deliver a homogeneous, nanosized precursor. Unfortunately, the technological potential of mi-

* Corresponding author. Tel.: +65-874-2958; fax: +65-776-3604; e-mail: maswangj@leonis.nus.edu.sg.
[1] Tel.: +65-874-2924; fax: +65-779-1691; e-mail: chmganlm@leonis.nus.edu.sg.

00167-577X/98/$19.00
PII: S0167-577X(98)00034-2

croemulsion processing has been limited by the aggregation of precursor particles during the subsequent drying and calcination stages, although the particle size of microemulsion-derived precursors may easily be controlled to as small as a few nanometers. This also applies to almost all the other wet chemistry-based processing routes, i.e., many of them are able to deliver an ultrafine precursor, but not an ultrafine ceramic product powder simply due to the fact that the unwanted aggregation of powder particles is out of control when the precursor is retrieved, dried, and finally calcined. The occurrence of hard particle agglomerates adversely affects the sintering of a ceramic powder and may lead to the formation of microstructural defects in the sintered ceramic [18]. Their elimination often requires an additional post-calcination de-agglomeration step [19], such as by ultrasonic fragmentation, shear and ball millings, which cause an apparent contamination to the resulting ceramic powders. Therefore, it is important to prevent the aggregation of precursor particles in order to avoid the formation of hard agglomerates. One of the feasible techniques for this is to 'isolate' each precursor particle from contacting with each other by forming a thin organic layer on their surfaces. The organic additive may be removed from the ceramic phase when the precursor is calcined at an appropriate temperature.

In the present work, a novel microemulsion processing route has been used for the preparation of ultrafine lead zirconate precursor. Polyaniline was introduced into the microemulsion-derived precursor via an in-situ polymerisation of anilines in the nanosized reaction domains when lead oxalate and zirconium oxalate are coprecipitated in the microemulsion consisting of cyclohexane, NP5 + NP9 and an aqueous phase.

2. Experimental procedure

The starting materials used in the present work included: a high purity lead(II) nitrate (> 99.7%, J.T. Baker, USA), oxalic acid dehydrate (> 99.9%, J.T. Baker); hydrogen peroxide (30%, Merck, Germany), anilines (> 99%, Merck); a high purity zirconium oxynitrate solution (20 wt.% ZrO_2, MEL, Manchester, UK), a high purity cyclohexane (Ajax, Australia), and a mixed non-ionic surfactant consisting of poly(oxyethylene)$_5$ nonyl phenol ether and poly(oxyethylene)$_9$ nonyl phenol ether (NP5:NP9 weight ratio: 2:1, Albright and Wilson, Singapore).

The procedure of establishing a partial phase diagram at room temperature for the ternary system consisting of cyclohexane, NP5 + NP9 and an aqueous solution has been detailed elsewhere [17,20–23]. Partial phase diagrams at room temperature for two ternary systems were established. They both consisted of cyclohexane, NP5 + NP9, together with an aqueous phase containing 0.10 M $Pb(NO_3)_2$ + 0.10 M $ZrO(NO_3)_2$ + 4.5 M H_2O_2, or 0.30 M oxalic acid + 1.0 M HCl + 0.50 M freshly distilled anilines. Fig. 1a,b show the partial phase diagrams established at room temperature for the two ternary systems, respectively.

The concurrent coprecipitation of lead oxalate and zirconium oxalate and in-situ polymerisation of anilines were brought about by mixing via vigorously stirring for 48 h two compositions both consisting of 56.0 wt.% cyclohexane, 24.0 wt.% NP5 + NP9 and 20.0 wt.% aqueous phase containing 0.10 M $Pb(NO_3)_2$ + 0.10 M $ZrO(NO_3)_2$ + 4.5 M H_2O_2, and 0.30 M oxalic acid + 1.0 M HCl + 0.50 M freshly distilled anilines, respectively. As shown in Fig. 1a,b, these two compositions are within the respective microemulsion regions. It was observed that the mixture turned from colourless to light green initially, then dark green and finally dark brown. To retrieve the precipitates, the mixture was washed repeatedly using distilled ethanol to remove the oil and surfactant phases, and subsequently was washed using deionised water until no trace of chloride was detected. The resulting precursor appeared dark grey when dried in a vacuum oven at room temperature.

The as-dried precursor powder was characterised using thermogravimetric analysis (TGA2950, Du Pont Instruments) and differential thermal analysis (DTA1600, Du Pont Instruments) at a heating rate of 10°C per minute in air from room temperature up to 900°C. It was then calcined in air at various temperatures, up to 900°C, followed by phase analysis using a X-ray diffractometer (Cu-$K\alpha$, Philips PW1729). Crystallite sizes in the calcined $PbZrO_3$ powders were estimated on the basis of line broadening at half maximum of (221) peak. The calcined and uncalcined powders were also analysed using a FTIR

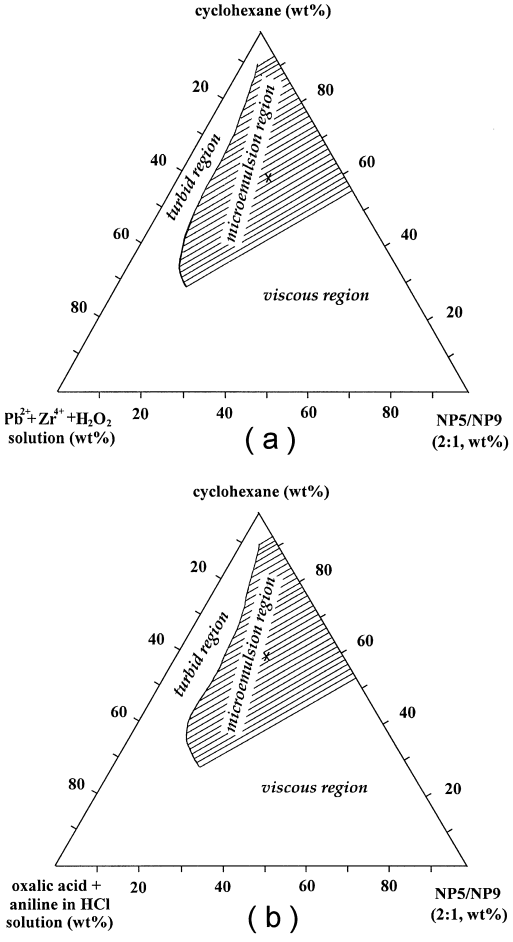

Fig. 1. Partial phase diagrams established at room temperature for the ternary systems consisting of cyclohexane, NP5 + NP9, and aqueous solution containing (a) 0.10 M $Pb(NO_3)_2$ + 0.10 M $ZrO(NO_3)_2$ + 4.5 M H_2O_2; and (b) 0.30 M oxalic acid + 1.0 M HCl + 0.50 M aniline.

spectrometer (Bio-Rad, FTS135) over the spectrum range from 4000 to 400 cm^{-1}, where the spectra were averaged over 64 scans with a nominal resolution of 2 cm^{-1} (KBr pellet). Particle/agglomerate size and size distribution of the calcined powders were measured by laser scattering technique (LA-910, Horiba). The discrete particle size was also estimated on the basis of the specific surface area obtained using a BET analyser (Nova 2000, Quantachrome). Transmission electron microscope (JEOL 100CX) and scanning electron microscopes (JEOL, JSM-35CF) and (Philips, FEG-XL30) were employed to analyse the particle/agglomerate morphology.

3. Results and discussion

When the two microemulsions, containing 0.10 M $Pb(NO_3)_2$ + 0.1 M $ZrO(NO_3)_2$ + 4.5 M H_2O_2, and 0.30 M oxalic acid + 1.0 M HCl + 0.50 M freshly distilled anilines, respectively, were mixed together, the following two reactions were expected to occur within the nanosized aqueous domains.

(i) Coprecipitation of lead oxalate and zirconium oxalate:

$$Pb(NO_3)_2 + ZrO(NO_3)_2 + 2H_2C_2O_4 + xH_2O = [PbC_2O_4 \cdot ZrOC_2O_4 \cdot xH_2O]\downarrow + 4HNO_3$$

(ii) Polymerisation of anilines:

As indicated by the gradual change in colour from an initially colourless to light green dark green and finally dark brown, it was believed that the polymerisation of anilines took place at a slower rate than the coprecipitation of lead oxalate and zirconium oxalate. In other words, the formation of oxalate precursor particles precede that of polyaniline in the nanosized aqueous droplets of the mixed microemulsion composition. This created an opportunity for each of the precursor particles to be coated with a polyaniline surface layer.

Fig. 2 is a bright-field TEM micrograph showing the as-dried oxalate precursor particles. They exhibit a rounded morphology and they are 15 to 30 nm in sizes. A loose coating layer was observed on the surface of these precursor particles and it was believed to be polyaniline. To confirm the existence of polyaniline, the as-dried precursor powder was analysed using a Bio-Rad FTIR spectrometer (FTS13). Fig. 3 shows the FTIR spectrum of the as-dried precursor and that of the powder calcined at 700°C for 1 h. The absorption at 822 cm^{-1} (CH o.p. bend), 1149 cm^{-1} (CH o.p. bend), 1291 cm^{-1} (CNC str.), and 1512 cm^{-1} (ring str.) clearly indicate the occurrence of polyaniline in the microemulsion-derived precursor [24,25]. Fig. 4 is a SEM micrograph showing the size and morphology of particle agglomerates in the as-dried oxalate precursor. The particle ag-

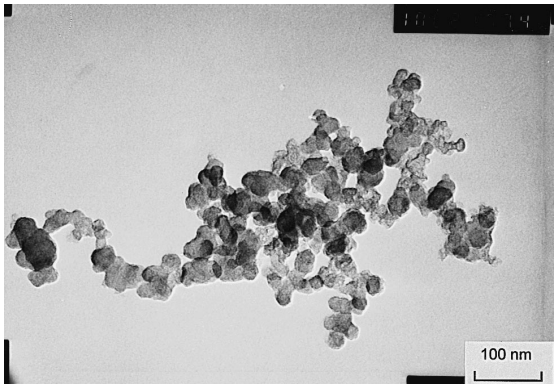

Fig. 2. A transmission electron micrograph of the as-dried precursor powder.

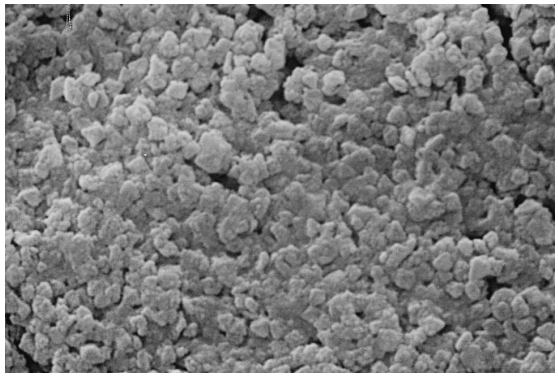

Fig. 4. A scanning electron micrograph of the as-dried precursor powder.

glomerates are 0.5 to 2.0 μm in sizes and they are well-dispersed. In support of the SEM observation, Fig. 5 shows the particle/agglomerate size distribution for the precursor powder, as measured by laser scattering technique. It covers a size range from 0.4 to 5.0 μm with an average size of 0.8 μm.

The thermal analysis results of the as-dried precursor powder are shown in Fig. 6 (TGA) and Fig. 7 (DTA), respectively. An initial fall in specimen weight is observed with increasing temperature from room temperature to 200°C, followed by a slow-down in weight loss rate over the temperature range from 200 to 280°C. The major fall in specimen weight occurs over a very narrow temperature range from 300 to 350°C. It is believed that the initial fall in specimen weight is due to the elimination of residual water and organic residuals. The major weight loss is believed to be a result of the decomposition of oxalates together with the further elimination of organic residuals in the precursor. To estimate the total weight loss in association with the elimination of polyaniline in the microemulsion-derived precursor, TG analysis was conducted on: (i) a pure polyaniline synthesised in an aqueous solution; and (ii) a polyaniline-free oxalate precursor. It was found that

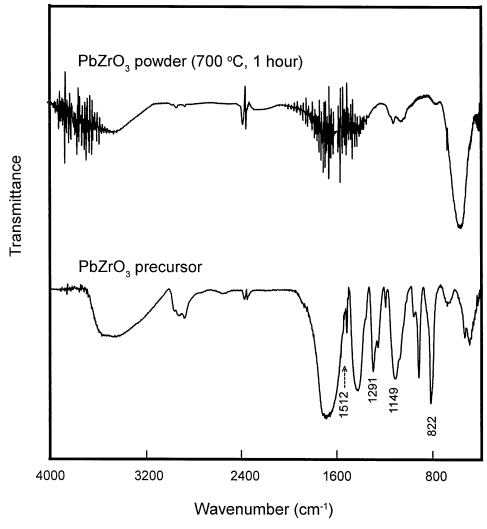

Fig. 3. The FTIR spectrum of the as-dried precursor and that of the powder calcined at 700°C for 1 h.

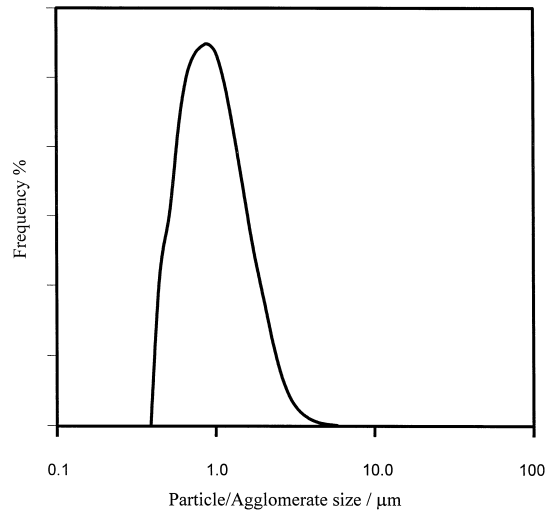

Fig. 5. Particle/agglomerate size distribution of the as-dried precursor powder.

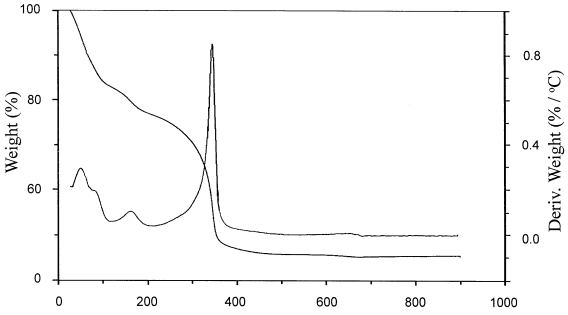

Fig. 6. TGA trace at a heating rate of 10°C/min in air for the as-dried precursor.

polyaniline exhibits a major weight loss over the temperature range of 350 to 520°C, which agrees well with the established decomposition temperature of polyaniline. It was also observed that the weight loss of polyaniline-free oxalate precursor was completed at temperatures below 350°C. It is therefore believed that the weight loss at temperatures above 350°C in Fig. 6 is due to the decomposition of polyaniline in the microemulsion-derived oxalate precursor. On the basis of this, a total of ~4 wt.% polyaniline was estimated.

As shown in Fig. 7, the microemulsion-derived oxalate precursor exhibits a small endothermic peak at ~180°C, together with a large, broadened exothermic peak extending from 330 to 440°C. The small endothermic peak corresponds to a noticeable fall in specimen weight over the same temperature range as shown in Fig. 6. Similarly, the broadened exothermic peak covers the temperature range of the major weight loss from 300 to 350°C, although it peaks at 370°C. This is a result of the decomposition of oxalates and the subsequent crystallisation of lead and zirconium oxides.

To study the phase development with increasing calcination temperature, the as-dried oxalate precursor was calcined for 1 h in air at 700, 800 and 900°C, respectively, followed by phase analysis using XRD at room temperature. Fig. 8 shows the XRD patterns for the powders calcined at these temperatures, indicating that a high percentage of orthorhombic $PbZrO_3$ was obtained at a calcination temperature as low as 700°C. This is ~100°C lower than that normally required for the formation of lead zirconate via either solid state reaction of mixed oxides or conventional coprecipitation [11,26]. Using Cohen's method of least-squares refinement [27], the lattice constants of the microemulsion-derived lead zirconate calcined at 800°C for 1 h are estimated as $a = 8.242$ Å, $b = 11.813$ Å and $c = 5.903$ Å. These

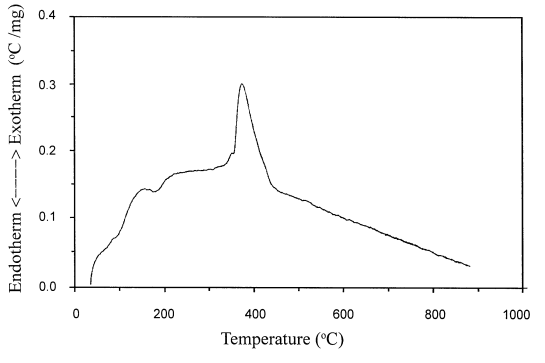

Fig. 7. DTA trace at a heating rate of 10°C/min in air for the as-dried precursor.

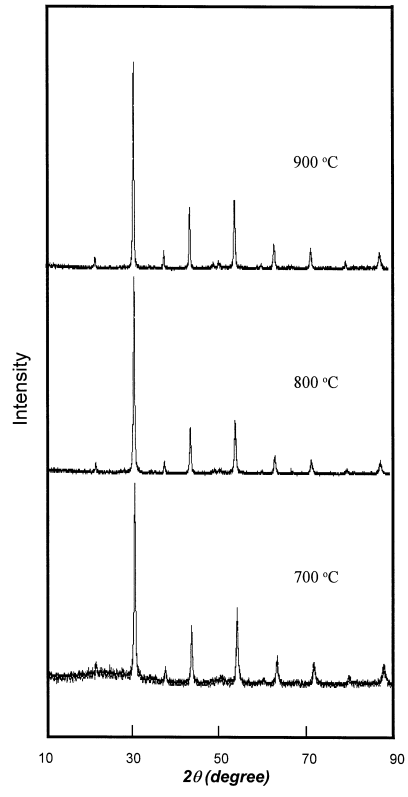

Fig. 8. XRD traces of the $PbZrO_3$ powders calcined for 1 h at 700, 800 and 900°C, respectively.

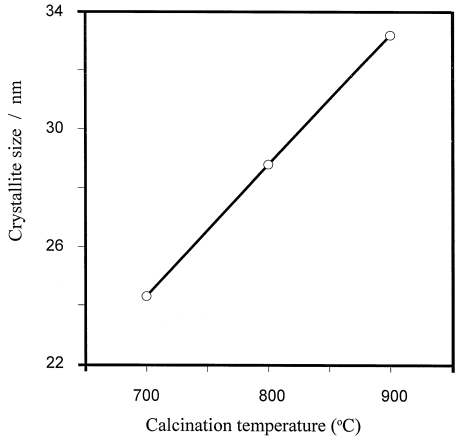

Fig. 9. The average crystallite size estimated on the basis of peak (221) broadening as a function of calcination temperature.

values are in good agreement with the data of ICDD PDF for lead zirconate (Card No. 35-0739). As expected, the average crystallite size of lead zirconate increases with increasing calcination temperature. Fig. 9 plots the average crystallite size, obtained using Scherrer equation [28] on the basis of XRD line broadening of peak (221), as a function of calcination temperature from 700 to 900°C.

The particle size distributions of the lead zirconate powder after calcination at 800°C for 1 h are shown in Fig. 10. The size curve on the righthand side was obtained when the powder was measured

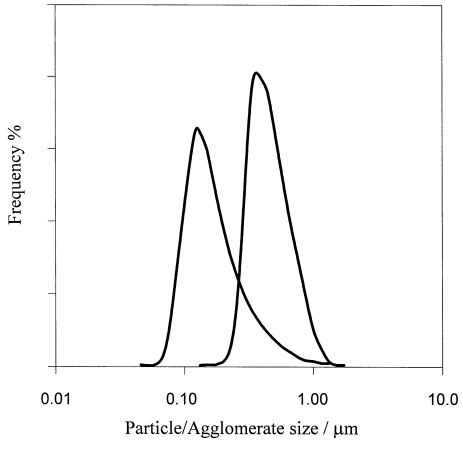

Fig. 10. The particle/agglomerate size distributions of the powder calcined at 800°C for 1 h. The curve on the righthand side was obtained when the powder was not subjected to any ultrasonic dispersion and that on the left hand side was obtained after the powder was ultrasonically dispersed for 5 min in distilled water.

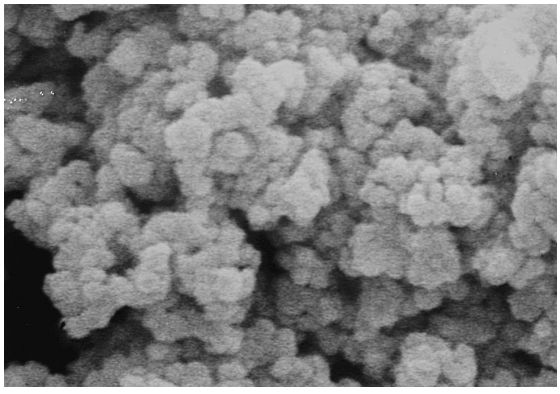

Fig. 11. A SEM micrograph showing the powder calcined at 800°C for 1 h.

without being subjected to any ultrasonication treatment and that on the left hand side was obtained after the powder had been ultrasonically dispersed in distilled water for 5 min. Therefore, the difference between them serves an indication on whether the particle agglomerates in the lead zirconate powder calcined at 800°C for 1 h can be easily eliminated by a conventional ultrasonic stirring. As expected, there is an apparent shift in particle size distribution towards the lower size range when the calcined lead zirconate powder was ultrasonicated for 5 min. In particular, the average particle size was shifted from 400 nm to 120 nm. It is thus believed that these sizes represent the agglomerate size distribution in the calcined lead zirconate powder, rather than the discrete particle size distribution. This is supported by the SEM micrograph in Fig. 11, which shows that particle agglomeration takes place although the dis-

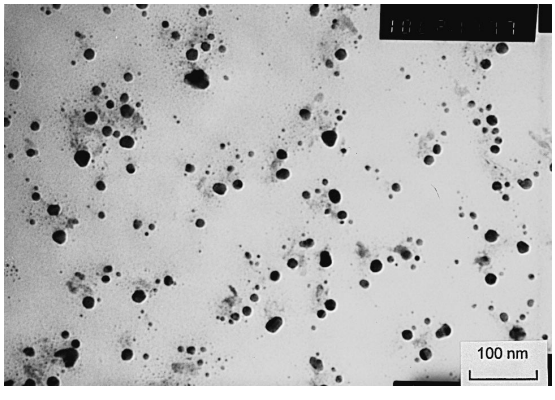

Fig. 12. A TEM micrograph showing the powder particles calcined at 800°C for 1 h.

crete particles are very small and exhibit a more or less spherical morphology.

As illustrated by the TEM micrograph shown in Fig. 12, most of the lead zirconate particles calcined at 800°C for 1 h are in the range of 10 to 20 nm although there is a small percentage of relatively larger crystallites. In support of the occurrence of nanosized lead zirconate particles in the powder, a BET specific surface area of 60.02 m^2/g was measured. This corresponds to an average particle size of 12.6 nm, as estimated by assuming that the powder particles are monosized spheres.

4. Conclusions

A lead zirconate powder of nanosized particles has been synthesised via a microemulsion processing route in the ternary system consisting of cyclohexane, NP5 + NP9 and an aqueous phase. A small amount (~4 wt.%) of polyaniline was retained in the microemulsion-derived oxalate precursor by an in-situ polymerisation in the nanosized aqueous domains when lead oxalate and zirconate oxalate were coprecipitated. The in-situ polymerisation of anilines on the surface of oxalate particles resulted in the formation of a well-dispersed precursor powder. Upon calcination at 800°C, the microemulsion-derived oxalate precursor led to the formation of an ultrafine lead zirconate powder, which was characterised for various powder characteristics.

Acknowledgements

This work was supported by research grants RP970609 and RP960692 from the National University of Singapore. The authors wish to thank Ms. Wan Dongmei and Miss Looy Yin Fong Eunice for their assistance in characterising the powders using SEM and TEM.

References

[1] B. Jaffe, W.R. Cook, H. Jaffe, Piezoelectric Ceramics, Academic Press, London, 1971, p. 123.
[2] G.H. Haertling, Ferroelectrics 75 (1987) 25.
[3] O.I. Prokopalo, E.G. Fesenko, M.A. Malitskaya, Y.M. Popov, V.G. Smotrakov, Ferroelectrics 18 (1978) 99.
[4] S.A. Gridnev, N.G. Pavlova, V.V. Gorbatenko, L.A. Shuvalov, Ferroelectrics 134 (1992) 365.
[5] H. Kamataki, T. Matsumoto, Y. Kawamura, (Fuji Electric), Japan Kokai Tokkyo Koho JP (Japan Patent No.) 02,272,781 [90,272,781], 7 November 1990.
[6] T. Oversluizen, G. Watson, Nucl. Instr. Meth. Phys. Res., Sect. A 246 (1986) 787.
[7] Y. Yamashita, S. Toshida, M. Harada, T. Takahashi (Toshiba), Japan Kokai Tokkyo Koho JP (Japan Patent No.) 61,129,888 [86,129,888], 17 June 1986.
[8] R. Watton, F. Ainger, S. Porter, D. Pedder, J. Gooding, Proc. SPIE-Int. Soc. Opt. Eng. 510, 139 (1984) (Pub. 1985) (Infrared Technol. 10).
[9] N. Ichinose, Kogyo Reametaru 80 (1993) 67.
[10] K. Singh, Ferroelectrics 94 (1994) 433.
[11] C.M. Jimenez, G.F. Arroyo, L.D.O. Guillen, P. Vincenzini (Eds.), Ceramic Powders, Elsevier, Amsterdam, 1983, 565 pp.
[12] E.E. Oren, E. Taspinar, A.C. Tas, J. Am. Ceram. Soc. 80 (1997) 2714.
[13] H. Cheng, J. Ma, B. Zhu, Y. Cui, J. Am. Ceram. Soc. 76 (1993) 625.
[14] S.S. Sengupta, L. Ma, D.L. Adler, D.A. Payne, J. Mater. Res. 10 (1995) 1345.
[15] M. Boutonnet, J. Kizling, P. Stenius, G. Maire, Coll. Surf. 5 (1982) 209.
[16] S. Bandow, K. Kimura, K. Kon-no, A. Kitahara, Jpn. J. Appl. Phys. 26 (1987) 713.
[17] J. Fang, J. Wang, S.-C. Ng, L.-M. Gan, C.-H. Chew, Ceram. Int. (1997) in press.
[18] K. Kendall, N.McN. Alford, J.D. Birchall, Proc. Br. Ceram. Soc. 37 (1986) 255.
[19] E. Jorge, T. Chartier, P. Boch, J. Am. Ceram. Soc. 73 (1990) 2552.
[20] J. Fang, J. Wang, S.C. Ng, C.H. Chew, L.M. Gan, Nanostruct. Mater. 8 (1997) 499.
[21] L.M. Gan, L.H. Zhang, H.S.O. Chan, C.H. Chew, B.H. Loo, J. Mater. Sci. 31 (1996) 1071.
[22] G.K. Lim, J. Wang, S.C. Ng, L.M. Gan, Mater. Lett. 28 (1996) 431.
[23] L.M. Gan, H.S.O. Chan, L.H. Zhang, C.H. Chew, B.H. Loo, Mater. Chem. Phys. 37 (1994) 263.
[24] N.S. Sariciftci, H. Kuzmany, H. Neugebauer, A. Neckel, J. Chem. Phys. 92 (1990) 4530.
[25] I. Harada, Y. Furukawa, F. Ueda, Synth. Metals 29 (1989) E303.
[26] S. Li, R.A. Condrate, S.D. Jang, R.M. Spriggs, J. Mater. Sci. 24 (1989) 3873.
[27] B.D. Cullity, Element of X-ray Diffraction, Addison-Wesley, Reading, MA, 1978, 363 pp.
[28] H.P. Klug, L.E. Alexander, X-ray Diffraction Procedures for Polycrystalline and Amorphous Materials, Wiley, New York, 1954, pp. 491–538.

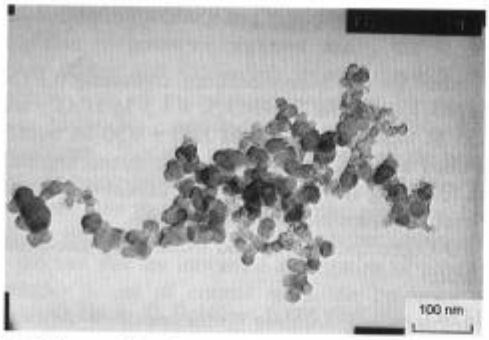

Fig. 2. A transmission electron micrograph of the as-dried precursor powder.

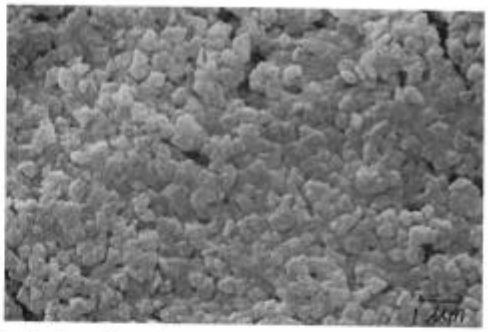

Fig. 4. A scanning electron micrograph of the as-dried precursor powder.

glomerates are 0.5 to 2.0 μm in sizes and they are well-dispersed. In support of the SEM observation, Fig. 5 shows the particle/agglomerate size distribution for the precursor powder, as measured by laser scattering technique. It covers a size range from 0.4 to 5.0 μm with an average size of 0.8 μm.

The thermal analysis results of the as-dried precursor powder are shown in Fig. 6 (TGA) and Fig. 7 (DTA), respectively. An initial fall in specimen weight is observed with increasing temperature from room temperature to 200°C, followed by a slow-down in weight loss rate over the temperature range from 200 to 280°C. The major fall in specimen weight occurs over a very narrow temperature range from 300 to 350°C. It is believed that the initial fall in specimen weight is due to the elimination of residual water and organic residuals. The major weight loss is believed to be a result of the decomposition of oxalates together with the further elimination of organic residuals in the precursor. To estimate the total weight loss in association with the elimination of polyaniline in the microemulsion-derived precursor, TG analysis was conducted on: (i) a pure polyaniline synthesised in an aqueous solution; and (ii) a polyaniline-free oxalate precursor. It was found that

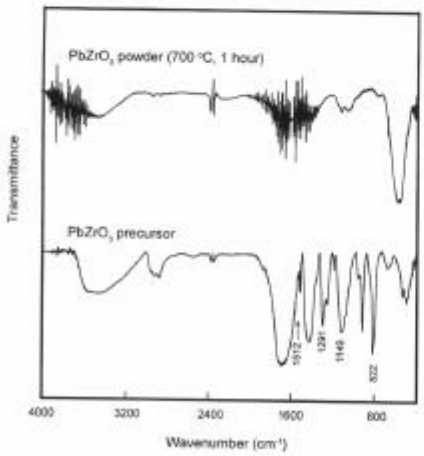

Fig. 3. The FTIR spectrum of the as-dried precursor and that of the powder calcined at 700°C for 1 h.

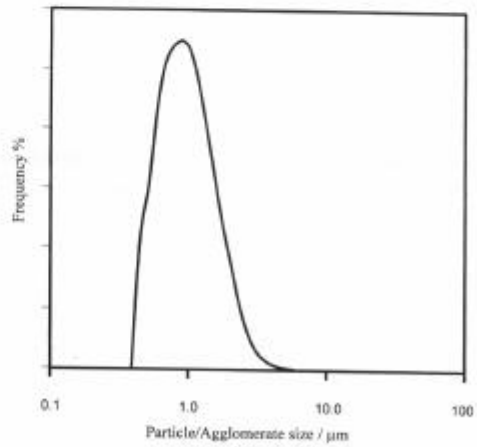

Fig. 5. Particle/agglomerate size distribution of the as-dried precursor powder.

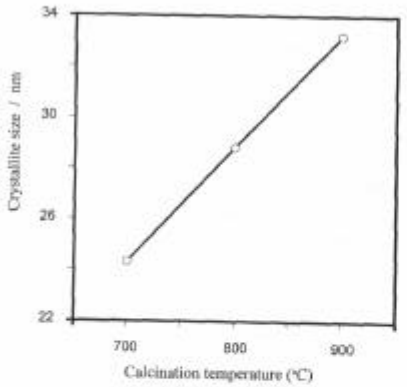

Fig. 9. The average crystallite size estimated on the basis of peak (221) broadening as a function of calcination temperature.

values are in good agreement with the data of ICDD PDF for lead zirconate (Card No. 35-0739). As expected, the average crystallite size of lead zirconate increases with increasing calcination temperature. Fig. 9 plots the average crystallite size, obtained using Scherrer equation [28] on the basis of XRD line broadening of peak (221), as a function of calcination temperature from 700 to 900°C.

The particle size distributions of the lead zirconate powder after calcination at 800°C for 1 h are shown in Fig. 10. The size curve on the righthand side was obtained when the powder was measured

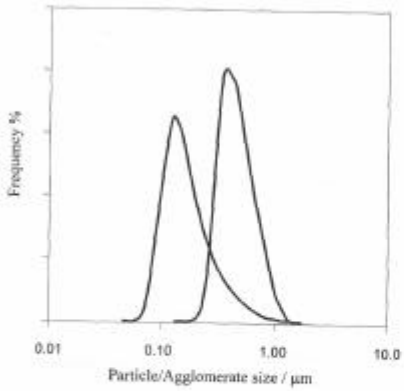

Fig. 10. The particle/agglomerate size distributions of the powder calcined at 800°C for 1 h. The curve on the righthand side was obtained when the powder was not subjected to any ultrasonic dispersion and that on the left hand side was obtained after the powder was ultrasonically dispersed for 5 min in distilled water.

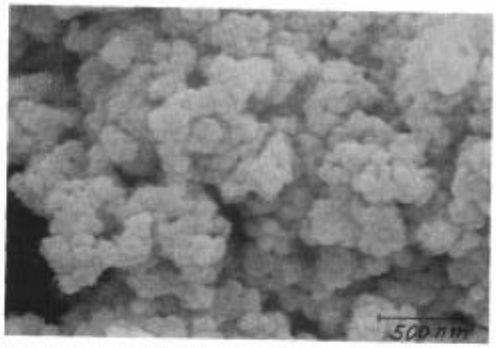

Fig. 11. A SEM micrograph showing the powder calcined at 800°C for 1 h.

without being subjected to any ultrasonication treatment and that on the left hand side was obtained after the powder had been ultrasonically dispersed in distilled water for 5 min. Therefore, the difference between them serves an indication on whether the particle agglomerates in the lead zirconate powder calcined at 800°C for 1 h can be easily eliminated by a conventional ultrasonic stirring. As expected, there is an apparent shift in particle size distribution towards the lower size range when the calcined lead zirconate powder was ultrasonicated for 5 min. In particular, the average particle size was shifted from 400 nm to 120 nm. It is thus believed that these sizes represent the agglomerate size distribution in the calcined lead zirconate powder, rather than the discrete particle size distribution. This is supported by the SEM micrograph in Fig. 11, which shows that particle agglomeration takes place although the dis-

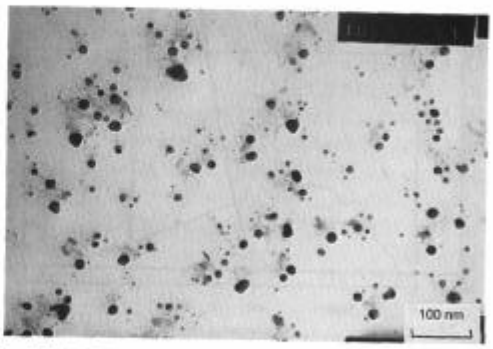

Fig. 12. A TEM micrograph showing the powder particles calcined at 800°C for 1 h.